

RSC Advances



This is an *Accepted Manuscript*, which has been through the Royal Society of Chemistry peer review process and has been accepted for publication.

Accepted Manuscripts are published online shortly after acceptance, before technical editing, formatting and proof reading. Using this free service, authors can make their results available to the community, in citable form, before we publish the edited article. This *Accepted Manuscript* will be replaced by the edited, formatted and paginated article as soon as this is available.

You can find more information about *Accepted Manuscripts* in the [Information for Authors](#).

Please note that technical editing may introduce minor changes to the text and/or graphics, which may alter content. The journal's standard [Terms & Conditions](#) and the [Ethical guidelines](#) still apply. In no event shall the Royal Society of Chemistry be held responsible for any errors or omissions in this *Accepted Manuscript* or any consequences arising from the use of any information it contains.



Journal Name

ARTICLE

Smart gold nanosensor for easy sensing of lead and copper ions in solution and using paper strips

Received 00th January 20xx,
Accepted 00th January 20xx

DOI: 10.1039/x0xx00000x

www.rsc.org/Peuli Nath,^{a,b} Ravi Kumar Arun,^{a,b} and Nripen Chanda^{a,b*}

A smart gold nanosensor, Au-TA-DNS is designed that can rapidly detect very low concentrations of Pb²⁺ and Cu²⁺ ions. The nanosensor develops visible blue colour in solution and on paper strips, because of the formation of nanoparticle aggregates upon binding with metal ions. Due to the presence of dansyl fluorophore, Au-TA-DNS also exhibits significant fluorescence quenching following Pb²⁺ and Cu²⁺ binding in aqueous medium, which is proportional to the concentration of ions. Both colorimetric and fluorometric analyses are very much selective for lead and copper ions with a detection limit of ≤ 10.0 ppb. The paper based sensing method has the advantage of cost-effectiveness and would be useful for wide range of field-test applications such as water quality monitoring process.

Introduction

Heavy metal pollution is a severe concern throughout the world because of their potential toxicity effects toward aquatic animals and humans.¹⁻³ Among various heavy metal toxins, lead and copper are two major toxic metal ions causing contamination from various sources like paint industry, lead pipes, brass fittings, galvanized steel pipes and corrosion of plumbing systems and medical implants.⁴⁻⁶ They are easily accumulated in human body as they cannot be detoxified by any chemical or biological processes. Accumulation of lead can cause kidney disorder, high blood pressure or irreversible brain damage in children aged 1-5 year old.^{7, 8} Likewise biochemically essential copper ion though needed for iron transportation, can also develop malignant tumour or Wilson disease if the copper level in serum is abnormally high.⁹ Though various optical and electrochemical methods have been developed to identify these toxic metal ions at tracer level (~ 10 ppb), existing methods have certain limitations such as cost effectiveness and requirements of complex equipment and sophisticated operations which are not accessible in remote areas for onsite real-time analysis. Well-established techniques like Atomic Absorption Spectrometry (AAS),

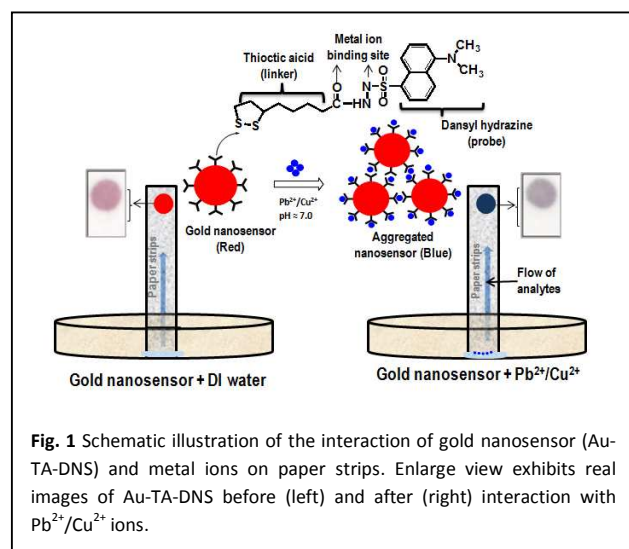
Inductively Coupled Plasma with Mass Spectrometry (ICP-MS) provide accurate detection of lead and copper, however they suffer from severe drawbacks, such as high time consumption, high-cost, and the requirement of sophisticated instrumentations.¹⁰ Similarly, electroanalytical method for these metal ions detection can give accurate determination with low detection limit, but it still requires a lab setting with bulk electrodes and electrochemical cell and also suffers from the interferences by co-deposition of other metals.^{11, 12} Other reliable approaches i.e. colorimetric and fluorometric methods are simple, inexpensive and widely employed in many applications including metal toxin detection with good sensing limit.¹³ However, most of the spectroscopic analyses are time consuming process and involved with safety issues as toxic chemicals are used directly during the operation.¹⁴

In order to circumvent the problems with toxic chemicals, functionalized gold nanoparticles (AuNPs) have been extensively used as potential sensor materials through colorimetric/fluorometric assays.¹⁵⁻¹⁹ AuNPs have high extinction coefficients and unique size-dependent optical properties.²⁰⁻²² When aggregate, the colour of AuNPs solutions changes from red to blue and the surface plasmon band broadens and shifts to longer wavelength. The analyte-induced aggregation of gold nanoparticles may also lead to the change in fluorescence intensity if fluorescence tag is present on the surface.²³ Based on these observations, AuNPs can be used as sensor materials to detect certain biologically relevant entities like toxic metal ions at fairly low concentrations. Indeed, various research groups have developed colorimetric and fluorometric sensing methods for various metal ions detection

^a Micro System Technology Laboratory, CSIR-Central Mechanical Engineering Research Institute, MG Avenue, Durgapur 713209, India. Fax: (0343)2546745; Tel: +91-9933034370; E-mail: n_chanda@cmeri.res

^b Academy of Scientific and Innovative Research (AcSIR), CSIR Campus, CSIR Road, Taramani, Chennai 600113, India.

Electronic Supplementary Information (ESI) available: See
DOI: 10.1039/x0xx00000x



using AuNPs.^{17-19, 24-26} In our previous work, functionalized AuNPs are used to detect arsenic and uric acid using paper-based microfluidic device.^{14, 27} Paper substrates have extensively been investigated in microfluidic research for its potential use in biosensor applications.²⁸⁻³¹ Due to the capillary based self-pumping action through fibres and pores, paper based device can execute a self-driven fluid flow with a steady flow-rate of 2-3 $\mu\text{l}/\text{min}$ for active transport through its micro-network.³² This slow but steady flow-rate allows a very low concentration of analytes to be retained in paper matrix for sufficient period of time for interaction with gold nanoparticles that can produce an intense signal in terms of precipitate or bands for analysis.

In this paper, we design a smart gold nanosensor, Au-TA-DNS with metal ion receptor cum fluorescent ligand that can rapidly detect Pb^{2+} and Cu^{2+} ions by distinct colorimetric and “turn-off” fluorescence sensing mechanisms in solution. When Pb^{2+} and Cu^{2+} ions are added to Au-TA-DNS solution, its fluorescence intensity decreases and colour changes markedly from red to blue as a result of ion-induced aggregations nanosensor. This distinct colour based response of Au-TA-DNS forms the platform of the present work to develop a sensor integrated paper based device that can be used for simple Pb^{2+} and Cu^{2+} ion detections. Au-TA-DNS exhibits immediate visible responses on paper strips even at very low level (≤ 10.0 ppb) ion concentration as demonstrated in Figure 1. To the best of our knowledge, this simple colorimetric sensing approach would be the first demonstration for lead and copper analysis on a piece of paper using gold nanosensor.

Experimental

Materials

Sodium tetrachloroaurate (III) dihydrate ($\text{NaAuCl}_4 \cdot 2\text{H}_2\text{O}$) was purchased from Alfa Aesar, England. Thioctic acid, Dansyl hydrazine, EDC (1-ethyl-3-[3-(dimethylamino)propyl]carbodiimide), Lead chloride were purchased from Sigma Aldrich, USA. NHS (N-hydroxysuccinimide) was procured from Fluka, USA. Sodium chloride and copper chloride were obtained from Merck, Germany. Other metal ions salts, reagents and solvents were obtained as analytical grades. Water was purified with a Milli-Q purification system.

Instrumentation

UV-vis absorption spectra were recorded on a Cary 60 Agilent technologies spectrophotometer at room temperature. Fluorescence spectra were taken on a Cary Eclipse fluorescence spectrometer. Size and charge were measured using NS500 (NanoSight) instrument. Field emission scanning electron microscopy (FESEM) was performed on a Zeiss Sigma HD electron microscope operated at an accelerating voltage of 200 kV. Centrifugation was performed on a SORVALL RC 6+ centrifuge. Fourier Transform Infra Red spectroscopy was carried on Jasco 4700 FT/IR instrument.

Synthesis of gold nanosensor (Au-TA-DNS)

Au-TA-DNS was prepared by a step-wise chemical conjugation of gold nanoparticles (AuNPs) with thioctic acid (TA) followed by fluorescent dansylhydrazine (DNS) molecules in presence of the coupling agents EDC-NHS. Briefly, 10.0 ml of citrate stabilized gold nanoparticles were prepared using 50.0 μl of 0.1M NaAuCl_4 and 5.0 mg sodium citrate dissolved in 1.0 ml DI water and stirred at 90°C. Colour of the solution gradually changed to bright red indicating the formation of gold nanoparticles (AuNPs). Next, 3.0 mg of thioctic acid dissolved in 1.0 ml methanol was added to 10.0 ml of citrate stabilized gold nanoparticles at pH 8.0. The mixture was stirred at room temperature overnight (8 hours). Unbound thioctic acid was removed by centrifuging the mixture at 9,000 rpm for 10 mins. Thioctic acid conjugated gold nanoparticle (Au-TA) pellet was dissolved in 5.0 ml water in order to perform second conjugation with dansylhydrazine. For this purpose, 200.0 μl each of 10 mM aqueous EDC (1-ethyl-3-[3-(dimethylamino)propyl]carbodiimide) and 10 mM aqueous NHS (N-hydroxysuccinimide) was added to the 5.0 ml Au-TA solution and stirred for 1 hour at room temperature. 7.0 mg dansylhydrazine dissolved in 1.0 ml DMSO-DI water was added to the above 5.0 ml Au-TA+EDC/NHS mixture. The mixture was stirred for 3 hours at room temperature. Excess dansylhydrazine was removed by centrifuging the mixture at 9,000 rpm for 10 mins. Finally, Au-TA-DNS was characterized by UV-vis, particle size analysis and field emission scanning electron microscopy techniques. IR spectrum was recorded to determine the dansylhydrazine conjugation with the thioctic acid via amide bond formation. The spectrum was blank subtracted and baseline corrected using software. The charge and size of Au-TA-DNS were evaluated to determine the stability of the nanosensor in solution. The average diameter was measured by NS500 in aqueous medium at 25°C. The

surface charge was determined by zeta potential measurement according to the manufacturer's instructions for measurement in high ionic strength media at 25°C. All measurements were performed in triplicate following dilution of nanoparticles by dispersing in high grade HPLC water (1.0 mg/ml). The values of size and charge are shown in Table S1. Further stability study was done in different pH solutions pH~4, pH~8 and in 1.0% NaCl solution and UV data were recorded by UV-vis spectrophotometer.

Pb²⁺ and Cu²⁺ detections by UV-vis and fluorescence techniques

A stock solution of Au-TA-DNS (5.0 mg/ml), and metal ions (0.1 mg/ml) were prepared in MilliQ water. Colorimetric detections of Pb²⁺ and Cu²⁺ ions were performed to determine the selectivity and lowest concentration detection ability of the nanosensor. During colorimetric detection, 0.1 ml of different concentrations of each metal ion (10, 1, 0.1, 0.01 and 0.001 ppm) was added into Au-TA-DNS solution (0.1 ml) to obtain the lowest limit of detection by naked eye. Selectivity of Pb²⁺ and Cu²⁺ for the synthesized gold nanosensor Au-TA-DNS was tested against various metal ions. 0.1ml of gold nanosensor in aqueous phase was mixed separately with 0.1ml of 0.01mg/ml (10 ppm) of various common metal ions Na(I), K(I), Cd(II),Mg(II), Cr(III), Fe(III), Hg(II) and Ca(II). Colour changes of the solutions were observed visually by naked eye. The corresponding UV-vis absorption spectra were also recorded. Following this experiment the selectivity test were also performed in straight paper strips where Au-TA-DNS was spotted and dried at one end of the strip and is kept vertically on a petridish having 10ppm solution of each metal ions. As the solutions moves upward due to capillary actions and touched the spotted red colour zone, differences in colour were observed and recorded using a digital camera. For fluorometric detection, similar protocols were followed but spectra were collected under fluorescence mode with a wavelength range 400 nm to 700 nm, excitation at 330 nm and slit width of 5 nm.

Analyses of Pb²⁺ and Cu²⁺ ions on paper strips

Analyses of Pb²⁺ and Cu²⁺ ions were performed on simple filter paper to test the practicality of gold nanosensor use. Whatman filter paper was used for the fabrication of straight and 'Y' shaped strips by micro-machining method carried out by CO₂ laser engraving system (VLS 2.30, Universal Laser Inc., USA) at 3 Watt. The engraved strip parameters were as follows: length (l) = 15.0 mm, width (w) = 3.0 mm (5.0 mm in case of straight strip) and height (h) = 0.1 mm (100 μm). The filter paper was soaked in warm HPLC grade water for 30 minutes to remove the impurities, if any. In straight strip experiment, one end was spotted with Au-TA-DNS and dried. Other end of the paper strip was kept vertically in petridishes in such a way that small part of the strip remains submerged in metal ion solutions of different concentrations. Due to capillary action,

metal solution moved up and reached to the spotted zone of the paper strip within few moments and colour change was observed (Fig. 1). For Y-shaped strip, Au-TA-DNS and each metal ion (Pb²⁺ and Cu²⁺) solution were kept in two petridishes, in which the extended arms of the strip were dipped. As soon as strip-arms touched into the respective solutions, the fluid started flowing into strip by capillary actions. When Au-TA-DNS solution interacts with metal ions, a bluish-black aggregate was formed at the interface within five minutes indicating the presence of metal ions.

Reversibility of gold nanosensor

To understand whether the metal ion binding is reversible, straight paper strips of Whatman filter paper were used. The paper strips were washed in warm water and dried to remove any kind of impurities. The gold nanosensor, Au-TA-DNS was spotted at one end of the paper strip (red colour). The strip was then kept vertically on a petridish containing 10 ppm Cu²⁺ or Pb²⁺ solution. As the ion solution moves up by capillary action and touched the red spotted zone, the colour turns blue after few minutes indicating the binding of metal ions to the Au-TA-DNS. The strip was then dried and again kept vertically in a petridish containing 0.1M EDTA (Ethylene-diaminetetraacetic acid) solution. As the EDTA solution moves upward to the spotted blue zone, it interacts with metal ion bound nanosensor and binds with the Cu ions, leaving the spotted zone red in colour because of free gold nanosensor. The paper strips with Au-TA-DNS (control), metal ion bound Au-TA-DNS and after EDTA treatment were characterized by UV-vis spectroscopy under solid state mode. The control and

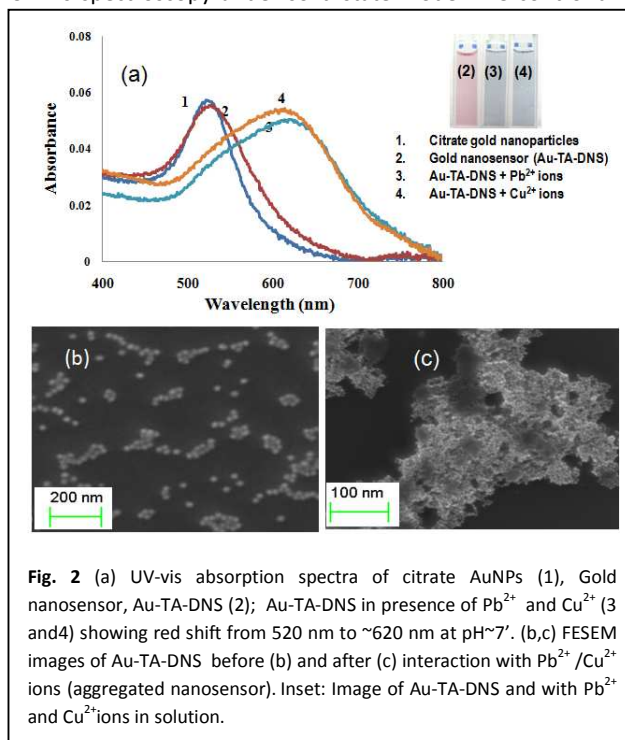


Fig. 2 (a) UV-vis absorption spectra of citrate AuNPs (1), Gold nanosensor, Au-TA-DNS (2); Au-TA-DNS in presence of Pb²⁺ and Cu²⁺ (3 and 4) showing red shift from 520 nm to ~620 nm at pH~7'. (b,c) FESEM images of Au-TA-DNS before (b) and after (c) interaction with Pb²⁺/Cu²⁺ ions (aggregated nanosensor). Inset: Image of Au-TA-DNS and with Pb²⁺ and Cu²⁺ ions in solution.

EDTA treated paper shows peak at $\sim 520\text{nm}$ indicating the reversibility of gold nanosensor after treatment with EDTA.

Results and discussion

Characterization and stability of gold nanosensor

Figure 1 demonstrates the schematic of gold nanosensor, Au-TA-DNS and its working principle for easy sensing of lead and copper ions on simple paper based strips. The detections of lead and copper are achieved by binding of metal ions with Au-TA-DNS that leads to the change in colour, UV-vis absorption profile and fluorescence intensity because of metal induced aggregation of gold nanosensor. The synthesis of nanosensor involves step-wise chemical conjugations of gold nanoparticles (AuNPs) with thioctic acid (TA) followed by fluorescent dansylhydrazine (DNS) molecules in presence of the coupling agents EDC and NHS. Each step was followed by hydrodynamic size and surface charge measurements (Table S1). The conjugation of dansylhydrazine with thioctic acid of AuNPs via amide bond formation ($\nu_{\text{NH}} = 3219\text{ cm}^{-1}$, $\nu_{\text{CO}} = 1643\text{ cm}^{-1}$) was confirmed by FTIR spectrum of the overall nanoconjugate shown in Fig. S1a. The UV-vis absorption spectra of Au-TA-DNS showed a broadening and a slight red shift of the plasmon resonance peak ($\sim 520\text{ nm}$) as compared to that of the unmodified AuNPs, indicating attachment of dansylhydrazine on the surface of AuNPs through thioctic acid linker (Fig. 2a).³³ The fluorescence spectrum of Au-TA-DNS as in Fig. 3, shows stable emission peak of DNS at 495 nm in water when excited at 330 nm . It should be noted that gold nanoparticles are known for quenching fluorescence when a fluorophore is placed directly on its surface.³⁴ Kang et. al. demonstrated that the fluorescent Cypate molecules bound directly onto the gold nanoparticle surface showed complete quenching of fluorescence property.³⁴ The level of quenching decreases as the fluorophore moved from the surface. Since the fluorescent dansylhydrazine is linked through thioctic acid, the quenching effect is not observed in Au-TA-DNS due to the presence of certain distance between DNS and AuNPs. After conjugation, Au-TA-DNS was treated with 1.0% NaCl and different pH media to monitor the stability through UV-vis spectroscopy as shown in Fig. S2. Negligible change in UV-vis band at $\sim 520\text{ nm}$ confirmed the excellent stability of the nanosensor. However, Au-TA-DNS became unstable in presence of Pb^{2+} and Cu^{2+} ions by showing visual colour change from red to blue due to inter-particle coupled plasmon resonance (Fig. 2, inset). This distinct visible colour change encourages us for the present study towards the detection of lead and copper ions using the gold nanosensor.

Affinity towards Pb^{2+} and Cu^{2+} ions

To explore the affinity of gold nanosensor towards $\text{Pb}^{2+}/\text{Cu}^{2+}$ ions, UV-vis and fluorescence techniques were employed to monitor the change in colour and fluorescence intensity in solution. Fig. 2 demonstrates the UV-vis spectra of Au-TA-DNS

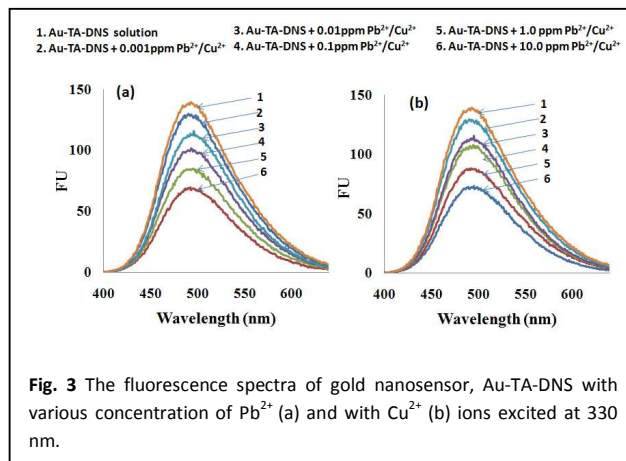
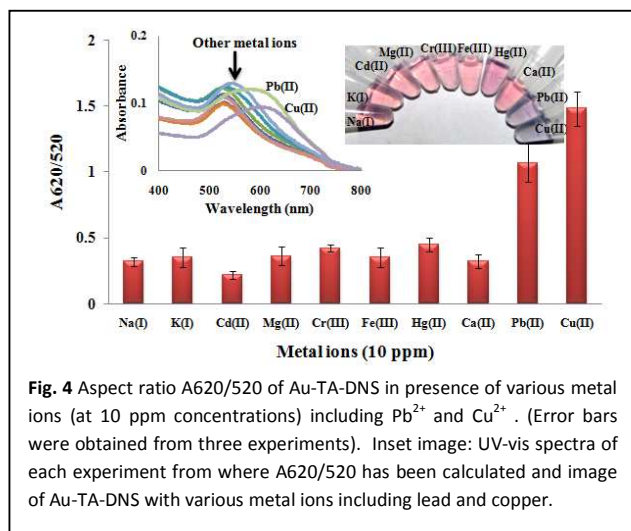


Fig. 3 The fluorescence spectra of gold nanosensor, Au-TA-DNS with various concentration of Pb^{2+} (a) and with Cu^{2+} (b) ions excited at 330 nm .

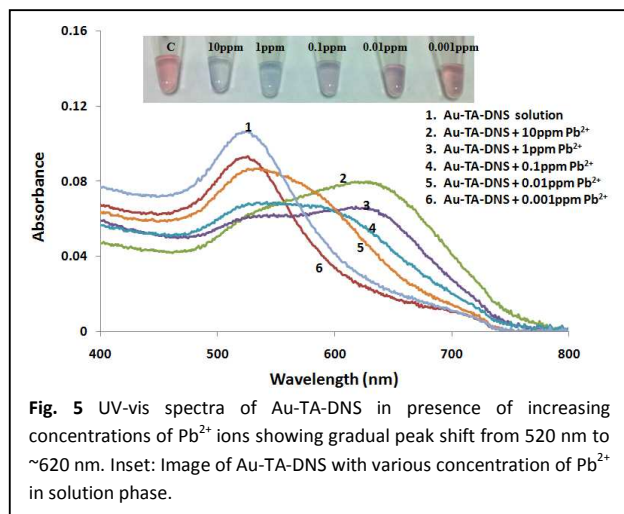
before and after treatment with lead and copper ions respectively at $\text{pH} \sim 7.0$. This pH was selected as Au-TA-DNS was stable due to electrostatic repulsion imposed by negative charge of nanosensor (-38.2 mV). The red shift in UV-vis wavelength ($\lambda_{\text{max}} = 520\text{ nm}$ to $\lambda_{\text{max}} \sim 620\text{ nm}$) indicates metal ion binding with Au-TA-DNS and formation of aggregates in solution. The metal ion binding may happen through the oxygen of $-\text{CO}-$ group and nitrogen attached to the sulfonyl group of dansylhydrazine that leads to the aggregation of nanosensor. The presence of the ν_{NH} at 3219 cm^{-1} and the red shift of the carbonyl ν_{CO} to 1586 cm^{-1} in the IR spectra indicate that the carbonyl O-atom and hydrazine N-atom are the coordination sites (Fig. S1b).³⁵ The gold nanosensor aggregation was confirmed by FE-SEM (Figure 2c) and particle size measurements (Table S1). This study shows the increase in hydrodynamic size of the nanosensor in presence of metal ions. Since Au-TA-DNS showed an emission band centred at about 495 nm in water ($\text{pH} = 7.0$), the detection ability was further explored by fluorescence measurement. It has been observed that the addition of Pb^{2+} and Cu^{2+} ions (10 ppm) caused two fold diminution of the typical dansyl-based fluorescence ($\lambda_{\text{max}} = 495\text{ nm}$, Fig. 3).^{36, 37} Of note, dansylhydrazine alone did not show any change in fluorescence intensity when same metal ions are added to the DNS (Fig. S3). The probable mechanism for the decrease in fluorescence intensity is due to the charge transfer from the fluorescent dansylhydrazine to the coordinated metal ion through $\text{Pb}/\text{Cu}-\text{O}$ and $\text{Pb}/\text{Cu}-\text{N}$ bonds.³⁷ This observation confirms that gold nanosensor has a strong affinity towards Pb^{2+} and Cu^{2+} ions and can work in “Turn off” approach for sensing applications.

Selectivity and sensitivity towards Pb^{2+} and Cu^{2+} ions

Next, the selectivity of Au-TA-DNS was tested in presence of various metal ions, Na (I), K(I), Cd(II), Mg (II), Cr(III), Fe(III), Hg(II) and Ca(II) including Pb^{2+} and Cu^{2+} . Each metal ion (10 ppm) was individually added to Au-TA-DNS solution and monitored through visual colour change and UV-vis



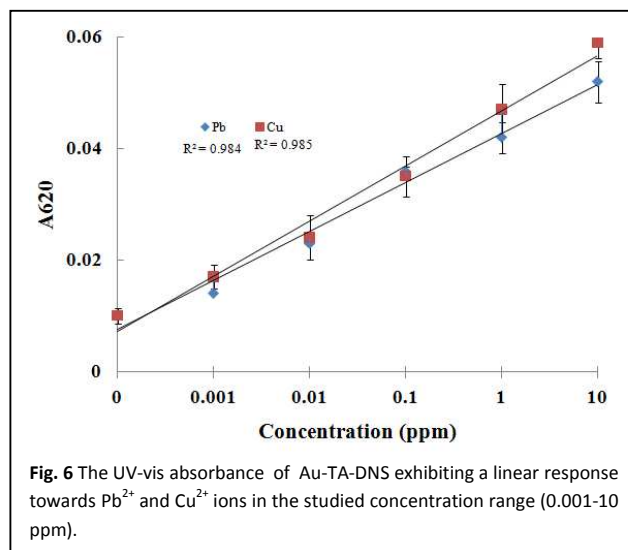
spectroscopy. Au-TA-DNS solution remains red against these interfering ions. As shown in Fig. 4, negligible differences were observed in UV-vis spectra (inset) and absorbance ratios (A_{620}/A_{520}) between the solutions containing 10 ppm of metal ions other than Pb^{2+} and Cu^{2+} . Similar results were also observed at the level of 0.10 ppm metal ion concentration. These studies demonstrate that other metal ions display slight to negligible interferences on the performance of gold nanosensor. In order to determine the sensitivity of Au-TA-DNS, various concentrations (10, 1, 0.1, 0.01, and 0.001 ppm) of lead and copper solutions were treated with Au-TA-DNS and monitored the progress of aggregation through UV-vis (Fig. 5) and fluorescence techniques (Fig. 3). With the increase of Pb^{2+}/Cu^{2+} concentrations, the colour of Au-TA-DNS solution gradually turned blue, suggesting an increase of the aggregation of AuNPs due to the binding of Pb^{2+}/Cu^{2+} to gold nanosensor (Fig. 5 and Fig S4). At concentrations 10, 1, 0.1, and 0.01 ppm, the absorption spectra show a gradual shift in wavelength (λ_{max}) from 520 to ~ 620 nm with a concomitant



growth of a new broad peak at ~ 620 nm. In case of 0.001 ppm concentration, this shift did not observe distinctly, which reveals the fact that the gold nanosensor is not sensitive below 0.01 ppm when UV-Vis technique is employed. Thus, sensitivity of the Au-TA-DNS was poor when visual colour change is considered; the nanosensor did not show significant colour difference in test tube at <0.01 ppm (Fig.5, inset). This is quite reasonable, because the number of metal ions (Pb^{2+} and Cu^{2+}) were very less to form the aggregates at this concentration and to show the blue colour in solution. This study clearly proves that colorimetric method has a certain cut-off limit in solution-phase analysis and is not suitable when the concentration of toxic ions is very low. However, the sensitivity at 0.001 ppm level was clearly visible when fluorescence technique employed. In fluorescence study, there were decrease in fluorescence intensities at 495 nm following the addition of increasing concentration of Pb^{2+} and Cu^{2+} ions starting from 0.001 ppm (Fig. 3). The decrease in peak intensity was clearly observed even at 0.001 ppm which was difficult in colorimetric analysis.

Discrimination between Pb^{2+} and Cu^{2+} ions using gold nanosensor

Since Au-TA-DNS detects both Pb^{2+} and Cu^{2+} ions, it is interesting to observe if the gold nanosensor can differentiate the detection process between these two ions. It has been observed that Au-TA-DNS gives blue colour immediately with Cu^{2+} ion (within few seconds) while it produces similar blue colour with Pb^{2+} ion within 2-3 minutes. When comparing the extent of aggregation of Au-TA-DNS through UV-Vis absorbance (A_{620}) measurements at different concentrations as shown in (Fig. 6), the A_{620} of Cu^{2+} was a little bit higher than Pb^{2+} indicating faster ion-induced aggregation and hence rapid colour change with Cu^{2+} ions compared to Pb^{2+} ions. We also investigated the colorimetric response of a mixture of Pb^{2+} and Cu^{2+} in solution. The colorimetric response was more obvious in case of Cu^{2+} ions than that of Pb^{2+} . These results



indicate that there is way to discriminate Cu^{2+} from Pb^{2+} ion

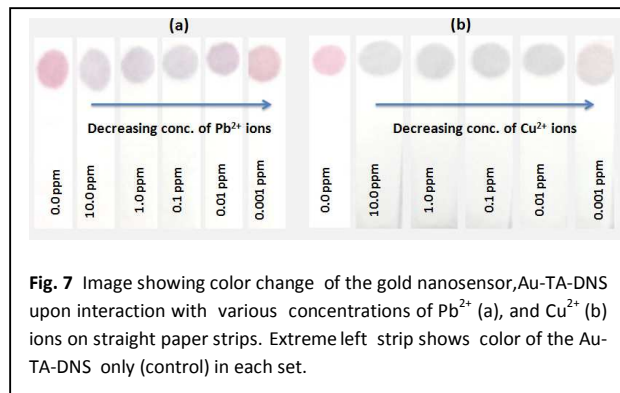


Fig. 7 Image showing color change of the gold nanosensor, Au-TA-DNS upon interaction with various concentrations of Pb^{2+} (a), and Cu^{2+} (b) ions on straight paper strips. Extreme left strip shows color of the Au-TA-DNS only (control) in each set.

using Au-Ta-DNS. Furthermore, the quantification of these metal ions is also possible from the linear response of Au-TA-DNS against various concentrations. Au-TA-DNS exhibits a linear response towards copper and lead ions in the studied concentration range (0.001-10 ppm) (Fig. 6). If the UV-vis profile is known for a lead or copper containing sample, the obtained absorbance value can be correlated to approximately estimate the ion concentration in that sample. Therefore, simultaneous detection and quantification of Pb^{2+} and Cu^{2+} ions could be achieved by careful monitoring the colour change and UV-vis profile of the nanosensor.

Pb^{2+} and Cu^{2+} ion sensing on paper strips

In order to evaluate the real application of the gold nanosensor, Au-TA-DNS for the detection of Pb^{2+} and Cu^{2+} ions in water, we checked its field test ability on simple paper strips. For this purpose, a straight paper strip made of Whatman filter paper was used to demonstrate the methodology as shown in Fig. 7. Like dipstick type devices, Au-TA-DNS was immobilized at one end as stationary-phase and the aqueous samples of Pb^{2+} and Cu^{2+} with various concentrations (10, 1, 0.1, 0.01, and 0.001 ppm) were flown separately through the strips as a single fluid for interaction. Due to capillary action, metal ion solution moved up and reached to the other end of the paper strip where Au-TA-DNS was spotted. The colorimetric responses (red to blue colour change) were clearly observed with each concentration, except 0.001 ppm of lead and copper. Like liquid phase study,

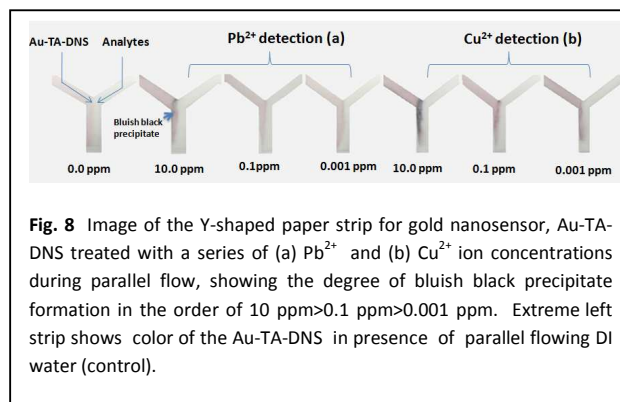
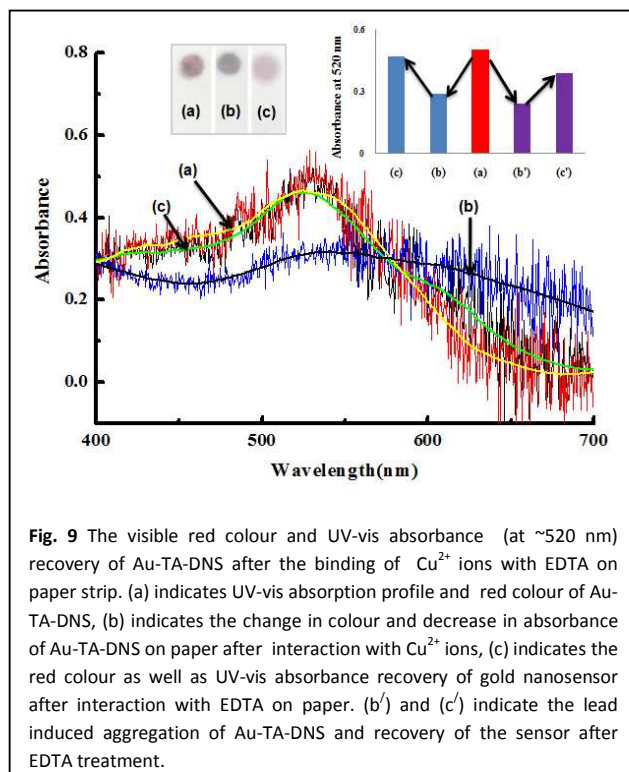


Fig. 8 Image of the Y-shaped paper strip for gold nanosensor, Au-TA-DNS treated with a series of (a) Pb^{2+} and (b) Cu^{2+} ion concentrations during parallel flow, showing the degree of bluish black precipitate formation in the order of 10 ppm > 0.1 ppm > 0.001 ppm. Extreme left strip shows color of the Au-TA-DNS in presence of parallel flowing DI water (control).

the paper based systems also show a gradual colour change with increasing metal ion concentrations. In Fig. 7, extreme left strip shows the blank study where no metal ions were added to Au-TA-DNS. The result of this study delineates the fact that like sensitive fluorescence mode of detection, the lowest detection limit cannot be reached beyond 0.010 ppm on paper strip. However, this study with single lateral flow of sample on a simple paper strip could easily be implemented to develop a dipstick type device for 0.010 ppm (10 ppb) level Pb^{2+} and Cu^{2+} ion detections. To realize Pb^{2+} and Cu^{2+} detection in presence of other common metal ions on paper strips, we prepared eight different solutions containing metal ion of Na (I), K(I), Cd(II), Mg (II), Cr(III), Fe(III), Hg(II) and Ca(II) at 10.0 ppm level and passed separately (except Pb^{2+} and Cu^{2+}) along with Au-TA-DNS. As shown in Fig. S5, like lead and copper, not a single metal ion shows any visible colour change when mixed with the nanosensor, showing high specificity of Au-TA-DNS for Pb^{2+} and Cu^{2+} ions on paper substrates.

In order to achieve very low sensitivity limit i.e. 0.001 ppm, we tried the parallel flow of two solutions, gold nanosensor and metal ions on Y-shaped paper strip, where both can be adequately mixed at their interface for interaction and produce an intense signal in terms of aggregates (Fig. 8). In microfluidic environment, the probability of mixing between gold based nanosensors and metal ions may increase many folds even at very low concentration to show the colour change in terms of aggregates at the confined interfacial zone or at the end of the channel.¹⁴ To execute this idea, a Whatman filter paper was cut into 'Y' shaped geometry with the following parameters: length (l) = 15.0 mm, width (w) = 3.0 mm and height (h) = 0.1 mm (100 μm). As shown in Fig. 8, gold nanosensor, Au-TA-DNS and metal ion solutions (Pb^{2+} and Cu^{2+}) were sent through two different arms by capillary actions as we demonstrated in our previous work.¹⁴ After meeting with metal ions, Au-TA-DNS formed a bluish-black aggregate within five minutes under microfluidic environments resulting in a distinct band at the interface of two solutions. The concentration of both metal ions was varied from 10 ppm to 0.001 ppm (1 ppb) and a clear deposition band was observed at the interface up to the concentration of 0.01 ppm (10 ppb). At 0.001 ppm, the band was faint to visualize with naked eye. However, this lowest detection limit can easily be confirmed by observing the interaction process for few more minutes as the band becomes distinctly visible with time. In a control study, DI water was sent through one of the arm of the strip

instead of metal ions containing sample, but no band or aggregate formation was observed while interacting with gold nanosensor on paper strips. Fig. 8 (a, b) compare the images of the Y-shaped strips for Au-TA-DNS treated with a series of Pb^{2+} and Cu^{2+} ion concentrations, such as 10 ppm, 0.1 ppm, and 0.001 ppm, showing the degree of deposition in the order of 10 ppm > 0.1 ppm > 0.001 ppm. Of note, while the concentration



of 0.001 ppm (1.0 ppb) is hardly detected in solution or straight paper strip as stated above, it is clearly seen in terms of aggregate deposition at the interface of the paper strip. This study suggests that nanosensor became highly sensitive when it flows with Pb^{2+} and Cu^{2+} ions in parallel fashion through a Y-shaped paper strip.

For a sensor to be widely used in the identification of specific analytes, the limit of reversibility is an important aspect. To understand whether the metal ion binding is reversible and the gold nanosensor can be reused for sensing the same, an external strong complexation agents (EDTA) was employed after aggregation process of Au-TA-DNS in the presence of Cu^{2+} and Pb^{2+} ions. In this regard, the changes in visible colour and UV-vis absorbance of Au-TA-DNS were observed in presence of 10.0 ppm of each of the metal ions followed by flowing 0.1 M EDTA solution on paper strip. As the carboxylic acid group can chelate with Pb^{2+} and Cu^{2+} ions, EDTA was used to study the reversibility of the visible red colour of the gold nanosensor.³⁸ It is clear from Fig. 9 that the colour and UV-vis absorbance of Au-TA-DNS after metal ion interaction (graph c) reaches close to its original position (graph a) with the continuous flow of EDTA solution through the paper strip. The recovery of red colour on paper strip also indicates that there is no effect of EDTA on the stability gold nanosensor (Fig 9, inset). The mechanism by which this process occurs is due to the formation of stable metal-EDTA complex that displaces the ions from the surface of Au-TA-DNS. This study indicates that

the nanosensor is reusable for detecting new Pb^{2+} and Cu^{2+} ions.

The performance of gold nanosensor was also explored after long term of storage at 4°C. It has been observed that Au-TA-DNS works well in solution and on paper substrate even after four to five weeks. This result demonstrates that the combination of Au-TA-DNS and paper substrate can develop a highly stable device for $\text{Pb}^{2+}/\text{Cu}^{2+}$ analysis like other reported state-of-art colorimetric sensors. Recently, a microfluidic sensor for lead detection has been developed by using a lead specific DNAzyme where syringe pumps, optical and electronic components were used as ancillary parts of the system.³⁹ The benefit associated with the present paper strip design is that this system can easily overcome the needs of expensive instrumental components and problems of toxic chemicals usages which essentially hamper the miniaturization of any practical sensing systems. The present paper strip can provide self-pumping of small volume of sample solution with stable flow rates to run the device for toxic metal analysis. Nevertheless, laminar mode of flow on thin paper strips (100 μm) also minimizes the fluids crossover to achieve stable deposition of nanosensor-metal ions aggregates at the interfacial zone over a reasonable period of time. In this way, the process ensures the detection of $\text{Pb}^{2+}/\text{Cu}^{2+}$ ions in the form of a clear cut mark at the interface even if the concentration of ions in solution is significantly low.

Conclusions

In conclusion, we have developed a smart gold nanosensor, Au-TA-DNS for dual colorimetric and fluorometric sensing of $\text{Pb}^{2+}/\text{Cu}^{2+}$ ions at very low concentration level (1.0 ppb) in solutions. The nanosensor shows turn-off fluorescence signal and distinct colour change from red to blue after mixing with $\text{Pb}^{2+}/\text{Cu}^{2+}$ ions. The unique characteristics of Au-TA-DNS make the detection process rapid and sensitive as it relies on metal-induced inter-particles aggregation behaviour of nanoparticles. The nanosensor also displays visible colour change on paper strip after diffusive mixing with $\text{Pb}^{2+}/\text{Cu}^{2+}$ ions. The benefit of this technique is that the paper based substrate has been used for the development of strip type device, thus the overall system becomes portable, power-free, cost-effective and safe to use in field for metal ion detection. Because of this simplicity, the present technology proves its inherent capacity for the development of a completely miniaturized sensing device by removing many challenges we generally face in the existing sensors for metal ion detection. Since sensing of Pb^{2+} and Cu^{2+} ions using Au-TA-DNS is the main focus of this research, the quantitative estimation ability of this nanosensor has not been investigated in detail. The quantitative test along with analysis of real sample containing lead and copper ions using this sensor is kept as a scope of future work.

Acknowledgements

The authors thank Dr Pijush Pal Roy, Director and Dr. Nagahanumaiah, Head, Micro System Technology Laboratory, CSIR-CMERI, Durgapur for their encouragements. Support from DBT grant under project no. GAP-101612 is gratefully acknowledged. The authors also thank to Saurav Halder, Vijay for channel fabrication and members of the institute CRF facility for FESEM study.

References

1. J. E. Gall, R. S. Boyd and N. Rajakaruna, *Environmental monitoring and assessment*, 2015, **187**, 201.
2. L. Jarup, *British medical bulletin*, 2003, **68**, 167-182.
3. J. Liu and G. Lewis, *Journal of environmental health*, 2014, **76**, 130-138.
4. H. Kozłowski, P. Kolkowska, J. Watly, K. Krzywoszynska and S. Potocki, *Current medicinal chemistry*, 2014, **21**, 3721-3740.
5. C. Mason, *Australian journal of public health*, 1993, **17**, 296-298.
6. B. Toth, S. Veres, N. Bakonyi, E. Gajdos, M. Marozsan and L. Levai, *Journal of environmental biology / Academy of Environmental Biology, India*, 2012, **33**, 425-429.
7. M. Ahamed and M. K. Siddiqui, *Clinica chimica acta; international journal of clinical chemistry*, 2007, **383**, 57-64.
8. A. P. Neal and T. R. Guilarte, *Toxicology research*, 2013, **2**, 99-114.
9. F. Tisato, C. Marzano, M. Porchia, M. Pellei and C. Santini, *Medicinal research reviews*, 2010, **30**, 708-749.
10. J. R. Kalluri, T. Arbneshi, S. A. Khan, A. Neely, P. Candice, B. Varisli, M. Washington, S. McAfee, B. Robinson, S. Banerjee, A. K. Singh, D. Senapati and P. C. Ray, *Angewandte Chemie*, 2009, **48**, 9668-9671.
11. M. Govindhan, B.-R. Adhikari and A. Chen, *RSC Advances*, 2014, **4**, 63741-63760.
12. B. K. Jena and C. R. Raj, *Analytical chemistry*, 2008, **80**, 4836-4844.
13. H. Choi, J. H. Lee and J. H. Jung, *The Analyst*, 2014, **139**, 3866-3870.
14. P. Nath, R. K. Arun and N. Chanda, *RSC Advances*, 2014, **4**, 59558-59561.
15. P. C. Ray, H. Yu and P. P. Fu, *Journal of environmental science and health. Part C, Environmental carcinogenesis & ecotoxicology reviews*, 2011, **29**, 52-89.
16. Y.-W. Lin, C.-C. Huang and H.-T. Chang, *The Analyst*, 2011, **136**, 863-871.
17. C.-W. Liu, Y.-T. Hsieh, C.-C. Huang, Z.-H. Lin and H.-T. Chang, *Chemical communications*, 2008, 2242-2244.
18. T. Senapati, D. Senapati, A. K. Singh, Z. Fan, R. Kanchanapally and P. C. Ray, *Chemical communications*, 2011, **47**, 10326-10328.
19. D. A. Giljohann, D. S. Seferos, W. L. Daniel, M. D. Massich, P. C. Patel and C. A. Mirkin, *Angewandte Chemie*, 2010, **49**, 3280-3294.
20. R. Arvizo, R. Bhattacharya and P. Mukherjee, *Expert opinion on drug delivery*, 2010, **7**, 753-763.
21. C. A. Wathen, C. Caldwell, N. Chanda, A. Upendran, A. Zambre, Z. Afrasiabi, S. E. Chapaman, N. Foje, W. M. Leevy and R. Kannan, *Contrast media & molecular imaging*, 2014.
22. A. Zambre, N. Chanda, S. Prayaga, R. Almudhafar, Z. Afrasiabi, A. Upendran and R. Kannan, *Analytical chemistry*, 2012, **84**, 9478-9484.
23. C. C. Huang, Z. Yang, K. H. Lee and H. T. Chang, *Angewandte Chemie*, 2007, **46**, 6824-6828.
24. W. Zhao, M. A. Brook and Y. Li, *Chembiochem : a European journal of chemical biology*, 2008, **9**, 2363-2371.
25. E. M, S. A. Alex, N. Chandrasekaran and A. Mukherjee, *Analytical Methods*, 2014, **6**, 9554-9560.
26. S. I. Hughes, S. S. Dasary, A. K. Singh, Z. Glenn, H. Jamison, P. C. Ray and H. Yu, *Sensors and actuators. B, Chemical*, 2013, **178**, 514-519.
27. A. Kumar, A. Hens, R. K. Arun, M. Chatterjee, K. Mahato, K. Layek and N. Chanda, *The Analyst*, 2015, **140**, 1817-1821.
28. W. Zhao, M. M. Ali, S. D. Aguirre, M. A. Brook and Y. Li, *Analytical chemistry*, 2008, **80**, 8431-8437.
29. G. H. Chen, W. Y. Chen, Y. C. Yen, C. W. Wang, H. T. Chang and C. F. Chen, *Analytical chemistry*, 2014, **86**, 6843-6849.
30. H. Liu, X. Li and R. M. Crooks, *Analytical chemistry*, 2013, **85**, 4263-4267.
31. A. W. Martinez, S. T. Phillips and G. M. Whitesides, *Proceedings of the National Academy of Sciences of the United States of America*, 2008, **105**, 19606-19611.
32. R. K. Arun, S. Halder, N. Chanda and S. Chakraborty, *Lab on a chip*, 2014, **14**, 1661-1664.
33. N. Chanda, V. Kattumuri, R. Shukla, A. Zambre, K. Katti, A. Upendran, R. R. Kulkarni, P. Kan, G. M. Fent, S. W. Casteel, C. J. Smith, E. Boote, J. D. Robertson, C. Cutler, J. R. Lever, K. V. Katti and R. Kannan, *Proceedings of the National Academy of Sciences of the United States of America*, 2010, **107**, 8760-8765.
34. K. A. Kang, J. Wang, J. B. Jasinski and S. Achilefu, *Journal of nanobiotechnology*, 2011, **9**, 16.
35. H. J. Liu, Y. H. Hung, C. C. Chou and C. C. Su, *Chemical communications*, 2007, 495-497.
36. M. Cao, L. Jiang, F. Hu, Y. Zhang, W. C. Yang, S. H. Liu and J. Yin, *RSC Advances*, 2015, **5**, 23666-23670.
37. K. Kavallieratos, J. M. Rosenberg, W. Z. Chen and T. Ren, *Journal of the American Chemical Society*, 2005, **127**, 6514-6515.
38. Y. Cho, S. S. Lee and J. H. Jung, *The Analyst*, 2010, **135**, 1551-1555.
39. L. Zhao, T. Wu, J. P. Lefevre, I. Leray and J. A. Delaire, *Lab on a chip*, 2009, **9**, 2818-2823.